Journal of Assisted Reproduction and Genetics (2019) 36:229–239
https://doi.org/10.1007/s10815-018-1369-0

REPRODUCTIVE PHYSIOLOGY AND DISEASE

Treatment of female rhesus macaques with a somatostatin receptor antagonist that increases oocyte fertilization rates without affecting post-fertilization development outcomes

Alison Y. Ting[1] · Melinda J. Murphy[1] · Pablo Arriagada[2] · Jean-Pierre Gotteland[2,3] · Jon D. Hennebold[1,4]

Received: 5 July 2018 / Accepted: 5 November 2018 / Published online: 15 November 2018

Abstract

Purpose To determine the effects of PGL1001, a somatostatin receptor isoform-2 (SSTR-2) antagonist, on ovarian follicle development, oocyte fertilization, and subsequent embryo developmental potential in the rhesus macaque.

Methods Cycling female rhesus macaques ($N = 8$) received vehicle through one menstrual (control) cycle, followed by daily injections of PGL1001, a SSTR-2 antagonist, for three menstrual (treatment) cycles. Main endpoints include overall animal health and ovarian hormones (e.g., estradiol [E2], progesterone [P4], and anti-Müllerian hormone [AMH]), ovarian circumference, numbers of oocytes and their maturation status following controlled ovarian stimulation (COS), as well as oocyte fertilization and subsequent blastocyst rates that were assessed in control and PGL1001 treatment cycles. Circulating PGL1001 levels were assessed at baseline as well as 6, 60, and 90 days during treatment.

Results PGL1001 treatment did not impact overall animal health, menstrual cycle length, or circulating levels of ovarian hormones (E2, P4, and AMH) in comparison to vehicle treatment during natural cycles. PGL1001 treatment increased ($p < 0.05$) ovarian circumference and the day 8 to day 1 ratio of AMH levels ($p < 0.05$) during a COS protocol, as well as oocyte fertilization rates compared to the vehicle treatment interval. Blastocyst development rates were not significantly different between vehicle and PGL1001 treatment groups.

Conclusion Prolonged treatment with PGL1001 appears to be safe and does not affect rhesus macaque general health, menstrual cycle length, or ovarian hormone production. Interestingly, PGL1001 treatment increased the fertilization rate of rhesus macaque oocytes collected following ovarian stimulation.

Keywords Somatostatin receptor antagonist · Nonhuman primate · Follicle development · Oocyte · Embryo

Introduction

Most studies support the idea that women are born with a finite number of eggs (oocytes), which progressively decreases with age [1]. The vast majority of oocytes are present in the form of primordial follicles, which are comprised of a quiescent oocyte surrounded by a single layer of flattened, non-dividing pre-granulosa cells. During each menstrual cycle, multiple primordial follicles leave this quiescent state and are irreversibly directed to undergo follicle growth and development [2, 3].

Only one follicle typically becomes dominant and is destined to ovulate in primates, whereas the subordinate follicles are lost through the process of atresia. Current infertility treatments rely on the use of exogenous gonadotropins (follicle-

Electronic supplementary material The online version of this article (https://doi.org/10.1007/s10815-018-1369-0) contains supplementary material, which is available to authorized users.

✉ Jon D. Hennebold
henneboj@ohsu.edu

[1] Division of Reproductive & Developmental Sciences, Oregon National Primate Research Center, Oregon Health & Science University, Beaverton, OR, USA

[2] PregLem SA, Geneva, Switzerland

[3] Present address: ObsEva SA, Chemin des Aulx, 12 Plan-les-Ouates, 1228 Geneva, Switzerland

[4] Department of Obstetrics & Gynecology, Oregon Health & Science University, Portland, OR, USA

stimulating hormone, FSH; luteinizing hormone, LH) to stimulate further growth and development of existing antral follicles into large ovulatory follicles, which then can be aspirated to collect oocytes for fertilization and embryo development [4]. This strategy depends on sufficient numbers of growing follicles that are responsive to exogenous FSH and LH. Therefore, one of the rate-limiting steps in current infertility treatments is the number of primordial follicles that transition into FSH-responsive small antral follicles. In some women, the size of the growing pool is very small, resulting in a limited number of mature follicles available for aspiration. Other factors affecting the success of infertility treatments include oocyte quality, which defines subsequent fertilization and embryo development potential. Treatments that can stimulate primordial follicles to enter the growing stage or improve oocyte quality would theoretically increase the number of mature and fertilizable oocytes collected, as well as the likelihood of enhanced in vitro fertilization (IVF) and subsequent embryo development rates.

Somatostatin (SST), also known as growth hormone-inhibiting hormone, is a peptide hormone that is present in multiple systems including the central nervous system, pituitary, gastrointestinal tract, pancreas, thyroid, kidney, and ovary [5]. SST not only inhibits the secretion of several exocrine and endocrine hormones or peptides but also has anti-proliferative and anti-angiogenic effects [5]. Therefore, SST and synthetic analogues were evaluated as treatments for a variety of neuroendocrine tumors [6, 7], diabetic complications [8], and polycystic liver disease [9] as well as polycystic ovarian syndrome [10]. Five SST receptors (SSTR-1–5) were identified, all of which are G protein-coupled receptors [11] expressed in various tissues [12]. In the ovary, SSTR-2 and -5 are the major SSTR subtypes and were reported to be expressed in bovine and human granulosa cells [12, 13], as well as in oocytes and granulosa cells of primordial and growing follicles in rodents [14, 15].

Several studies have suggested a role of SST in ovarian function, including inhibition of follicle recruitment [16], steroidogenesis [17], and oocyte maturation [18], which may be the result of increased rates of follicle atresia [19]. Systemic SST treatment of rats during the peri-pubertal interval increased the number of the primordial (non-growing) follicles compared with untreated rats [16]. Conversely, blocking the ability of SST to act through SSTR-2 using an SSTR-2 selective antagonist increased the follicle transition from the non-growing pool into the growing pool in comparison to untreated mouse ovaries in vitro, suggesting a local control of SSTR signaling on initial follicle recruitment [14]. Similarly, systemic SST treatment caused follicle atresia in all phases of folliculogenesis, especially in large antral follicles [19], whereas blocking ovarian SSTR-2 signaling using a siRNA approach inhibited granulosa cell apoptosis in bovine primary granulosa cells [13]. These studies suggest that SST inhibits folliculogenesis and induces follicle atresia in rodents and bovine and these actions can be reversed by blocking SSTR-2 signaling, thereby promoting follicle recruitment and survival of growing follicles. Whether a similar effect of SSTR inhibition occurs in the primate ovary is unclear.

Female rhesus macaques and women share numerous similarities with regard to reproductive physiology, including a 28-day and mono-ovulatory menstrual cycle, comparable rates of folliculogenesis, and hormone profiles (e.g., similar circulating FSH, LH, estradiol [E2], and progesterone [P4] levels). Moreover, both species respond similarly to ovarian stimulation and have comparable IVF and embryonic development (i.e., blastocyst formation) rates [20–22]. Additionally, rhesus monkeys and humans share 99.7% sequence homology of the SSTR-2 receptor. Thus, the goal of the current study is to utilize the rhesus macaque to determine the effects of PGL1001, an SSTR-2 antagonist, on primate ovarian follicle development. Experiments were performed to evaluate whether systemic PGL1001 increases ovarian follicle recruitment, which in turn leads to the growth and development of more follicles following stimulation with exogenous hormones and a greater number of mature oocytes available for fertilization. Other endpoints include overall animal health and ovarian hormone production as well as oocyte fertilization and subsequent embryo developmental potential.

Materials and methods

Animals

The general care and housing of rhesus macaque monkeys (*Macaca mulatta*) was provided by the Division of Comparative Medicine at the Oregon National Primate Research Center (ONPRC) as previously described [23]. Animals were pair-caged in a temperature-controlled (22 °C) light-regulated (12L:12D) room and fed monkey chow twice a day and water ad libitum. The studies were conducted according to the National Institutes of Health Guide for the Care and Use of Laboratory Animals. All animal protocols and procedures were approved by ONPRC's Institutional Animal Care and Use Committee.

Young adult female rhesus macaques ($N = 8$; 4.5–7.0 years old) exhibiting regular menstrual cycles received vehicle and PGL1001 treatments sequentially in a longitudinal study to minimize inter-animal variability (Fig. 1). Beginning on day (D) 1–3 of Cycle 1, animals received daily vehicle treatment (subcutaneous [SC] q.d. sterile saline containing 0.001 N HCl and 2% heat-inactivated monkey serum; vehicle, Veh). Cycle D1 is defined as the first day of menses. All animals were subjected to a controlled ovarian stimulation protocol (COS; COS1) beginning of Cycle 2 and received no intervention in Cycle 3 (rest cycle). Beginning on D1–3 of Cycle 4, a SSTR-2

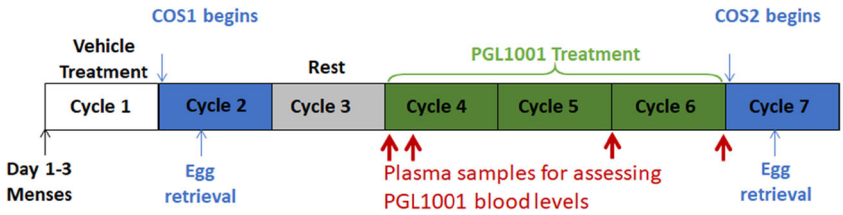

Fig. 1 Schematic of experimental design and timeline

antagonist (PGL1001; Preglem SA, Geneva, Switzerland) was administered SC daily at a dose of 0.4 mg/kg (dissolved in 2% DMSO and vehicle) to each animal for three consecutive months (Cycles 4–6). A second COS protocol (COS2) was performed at the beginning of Cycle 7 (started D2 to D4 after onset of menses). Preliminary PK studies revealed that both 0.4 and 2 mg/kg doses of PGL1001 are extremely well tolerated and safe in cynomolgus monkeys when administered twice a day for 3 months (data not shown). No side effects were observed. A 0.4 mg/kg dose of PGL1001 was selected for this study and is within the range of well-tolerated doses used in the cynomolgus macaque study (data not shown). Data for the previous Ki and IC50 studies in cynomolgus macaques are provided in Supplemental Table 1.

Blood samples for hormone analyses were collected every 3 days starting on D1 of the menstrual cycle during Cycles 1 and 4–6, and every day throughout the COS protocol in Cycles 2 (no drug) and 7 (3 months of continuous drug exposure). Additional blood samples were collected on D1 and D7 after the start of PGL1001 treatment as well as at the end of Cycle 5 and Cycle 6 to measure PGL1001 plasma concentrations by mass spectrometry (MPI Research, Mattawan, MI). In addition, menses and general animal well-being were monitored daily. Complete blood count (CBC) and blood chemistry tests were performed prior to (at the end of Cycle 3), during (D7 in Cycle 4), and at the end of PGL1001 treatment in Cycle 6.

Controlled ovarian stimulation and follicle aspiration

The controlled ovarian stimulation (COS) and follicle aspiration procedures were described previously [21, 24]. Briefly, beginning D1–4 of menses, monkeys received recombinant human (rh) FSH (30 IU, twice a day, IM) for 6 days, followed by rhFSH and rhLH (30 IU each, twice a day, IM) for 2 days (Merck & Co.-Organon, West Orange, NJ and Merck-Serono Reproductive Biology Institute, Rockland, MA; respectively). A GnRH antagonist (Antide, 1 mg/kg, SC; Salk Institute for Biological Studies, La Jolla, CA) was administered when circulating E2 levels were > 150 pg/ml to prevent a spontaneous ovulatory LH surge. On D8 of the COS protocol, a bolus of human chorionic gonadotropin (hCG; 1000 IU; Novarel, Ferring Pharmaceuticals, Parsippany, NJ) was administered to induce meiotic progression of oocytes. Thirty-six hours post-hCG, using a needle attached to a vacuum with pressure set at 80–120 mmHg, multiple antral follicles were aspirated by laparoscopy into a TALP-HEPES buffered solution (Sigma-Aldrich) with 0.3% bovine serum albumin (BSA, Sigma-Aldrich). During surgical procedures, OHSU IACUC-approved standard anesthesia protocols were carried out using ketamine, lidocaine with 1% epinephrine, O2, isoflurane, bupivacaine HCl, and buprenorphine, followed by a standard post-operative procedure using opioid analgesia (buprenorphine).

IVF and embryo culture

Following follicle aspiration, cumulus-oocyte-complexes (COCs) were briefly exposed to 1% hyaluronidase (Sigma-Aldrich) in TALP-HEPES with 0.3% BSA [24]. Cumulus-free oocytes were collected and grouped into the following meiotic stages: germinal vesicle (GV; failed to reinitiate meiosis), metaphase I (MI; GV breakdown), and metaphase II (MII; mature, presence of a polar body). Standard IVF was performed on all healthy oocytes as previously described [23, 24]. Briefly, oocytes were inseminated in 100-μl drops of TALP + 0.3% BSA with freshly collected sperm provided by the ONPRC Assisted Reproductive Technologies (ART) Core and cultured for 18 h. Oocytes/zygotes were then washed and transferred into Global Media with 10% Protein Supplement (LifeGlobal Group, LLC). Since IVF was performed instead of intra-cytoplasmic sperm injection, the precise timing of fertilization and the expected timing for the presence of pronuclei were unpredictable. Therefore, evidence of the first mitotic cell division (2-cell stage) was used as a measure of fertilization at 36 h post-IVF [24]. Because traditional IVF is performed in the current study, all collected healthy oocytes regardless of their maturation stage at collection were incubated overnight in the presence of sperm. Thus, 36 h post-IVF, zygotes that reached the 2-cell stage could be from fertilized MII oocytes (MII stage at collection) or collected MI or GV oocytes that reached the MII stage during IVF incubation. The number of 2-cell embryos and unfertilized MII oocytes were counted 36 h post-IVF. Embryos were cultured until blastocyst formation (~ 8 days) or developmental arrest. Oocyte maturation (MI + MII oocytes), fertilization (two-cell stage), and blastocyst formation rates (%) were determined. Oocyte maturation rate was calculated as the number of MI plus MII oocytes divided by the total number of oocytes (MII, MI, GV, and atretic) at oocyte collection. Fertilization rate was calculated as the number of 2-cell stage embryos divided by the number of cleaved embryos plus unfertilized MII oocytes at

36 h post-IVF. Blastocyst rate was calculated as the number of blastocysts divided by the number of fertilized oocytes (i.e., 2-cell embryos). To eliminate the effect of variable sperm quality from different donors on IVF and early embryonic development, sperm from the same donor was used for insemination of oocytes collected from different COS cycles of the same female rhesus macaque. In addition, each sperm donor has at least two full days of rest between each semen collection.

Ultrasound imaging

Ovarian ultrasound (US) was performed during Cycles 1–2 and 4–7 during early (D1–3; D1 being the first day of menses) and late (D7–10) follicular phase as described previously [25] using a GE Medical Systems Voluson 730 Expert Doppler ultrasound instrument (GE Healthcare, Waukesha, WI) with a 4D (3.3–9.1 MHz) and transabdominal probe. Ovarian size was not assessed during each COS cycle due to the dramatic increase in circumference that occurs as a consequence of the growth of multiple follicles in response to exogenous gonadotropins. Ovarian size, defined as the circumference of the US image with the longest axis [25], was measured using 4D View software (GE Healthcare). Ovarian size as measured by its circumference has been used for characterization of follicle size and dynamics in rhesus macaque ovaries and demonstrated to correlate with the number of antral follicles as well as the number of oocytes collected following COS protocol and oocyte aspiration [25]. Ovarian circumference in each animal was calculated as the average of the left and right ovary circumference at each time point.

Hormone analysis

Serum levels of E2, P4, and AMH were measured by the ONPRC Endocrine Technologies Support Core [26]. E2 and P4 were analyzed using a Roche cobas e411 automated clinical platform (Roche Diagnostics, Indianapolis, IN). The assay ranges for the E2 and P4 assays were 5–4300 pg/ml and 0.030–60 ng/ml, respectively. Intra- and inter-assay coefficient of variations (CV) for the steroid assays in the ETSC are consistently less than 7%. AMH was measured using ELISA with a commercial kit (AL-105; AnshLabs, Webster, TX) based on the manufacturer's instructions [27]. Intra-assay CVs for AMH ranged from 1.2 to 6.1% and inter-assay CV was 11.9% (n = 7). In addition, the ETSC includes an in-house nonhuman primate serum quality control pool with each assay.

Statistical analysis

Data are presented as the mean ± SEM. Statistical significance was determined using one-way repeated measures ANOVA and Student-Newman-Keuls post-hoc analysis (SigmaPlot 11.0; Systat Software, Inc., San Jose, CA, USA) for data comparison among different treatment time points. Two-way repeated measures ANOVA was performed for data with two measurements within the same treatment time point (i.e., early and late follicular phase). Difference was considered significant when $p < 0.05$.

Results

PGL1001 plasma concentration and overall animal health

The eight rhesus macaques assigned to the project completed the entire study protocol (seven menstrual cycles). PGL1001 plasma levels increased during the treatment interval and peaked at the end of cycle 6 (Supplemental Table 2). Maximum PGL1001 levels ranged between 85.7 ng/ml (73.6 nM) and 3200 ng/ml (2700 nM). All animals achieved a final circulating PGL1001 level that was above its Ki value 6.4 nM. Throughout the study, all animals were monitored closely by ONPRC veterinarians and trained animal care technicians daily, and no abnormalities were reported with regard to their food intake and urine and feces output, as well as activity and behavior. All animals also tolerated daily vehicle/PGL1001 injections and showed no signs of inflammation or negative outcomes at the injection site. No PGL1001-dependent effects on CBC and blood chemistry parameters were observed (data not shown).

Menstrual cyclicity and ovarian hormone production

All animals had menstrual cycle lengths through the vehicle treatment cycle that were similar to those from ONPRC historical records (average = 27 ± 1 days; range = 23 to 34 days, Fig. 2a). Through 3 cycles of PGL1001 treatment, the menstrual cycle length did not differ ($p > 0.05$) from that of the vehicle cycle (Fig. 2a). A mid-cycle rise in E2 followed by elevated P4, indicative of an ovulatory cycle, was observed in all animals during the vehicle and subsequent PGL1001 treatment cycles (cycles 4 through 6). Area under the curve assessment of E2 and P4 production demonstrated that their levels were not different ($p > 0.05$) between vehicle and PGL1001 treatment cycles (Fig. 2b and c). When measured at early or late follicular phase, serum AMH did not differ ($p > 0.05$) between the vehicle and any of the PGL1001 treatment cycles (Fig. 2d). However, late follicular AMH levels were lower ($p < 0.05$) than those observed during the early follicular phase in the vehicle and first cycle of PGL1001 treatment. A similar trend ($p < 0.1$) was observed in the second and third PGL1001 cycles (Fig. 2d).

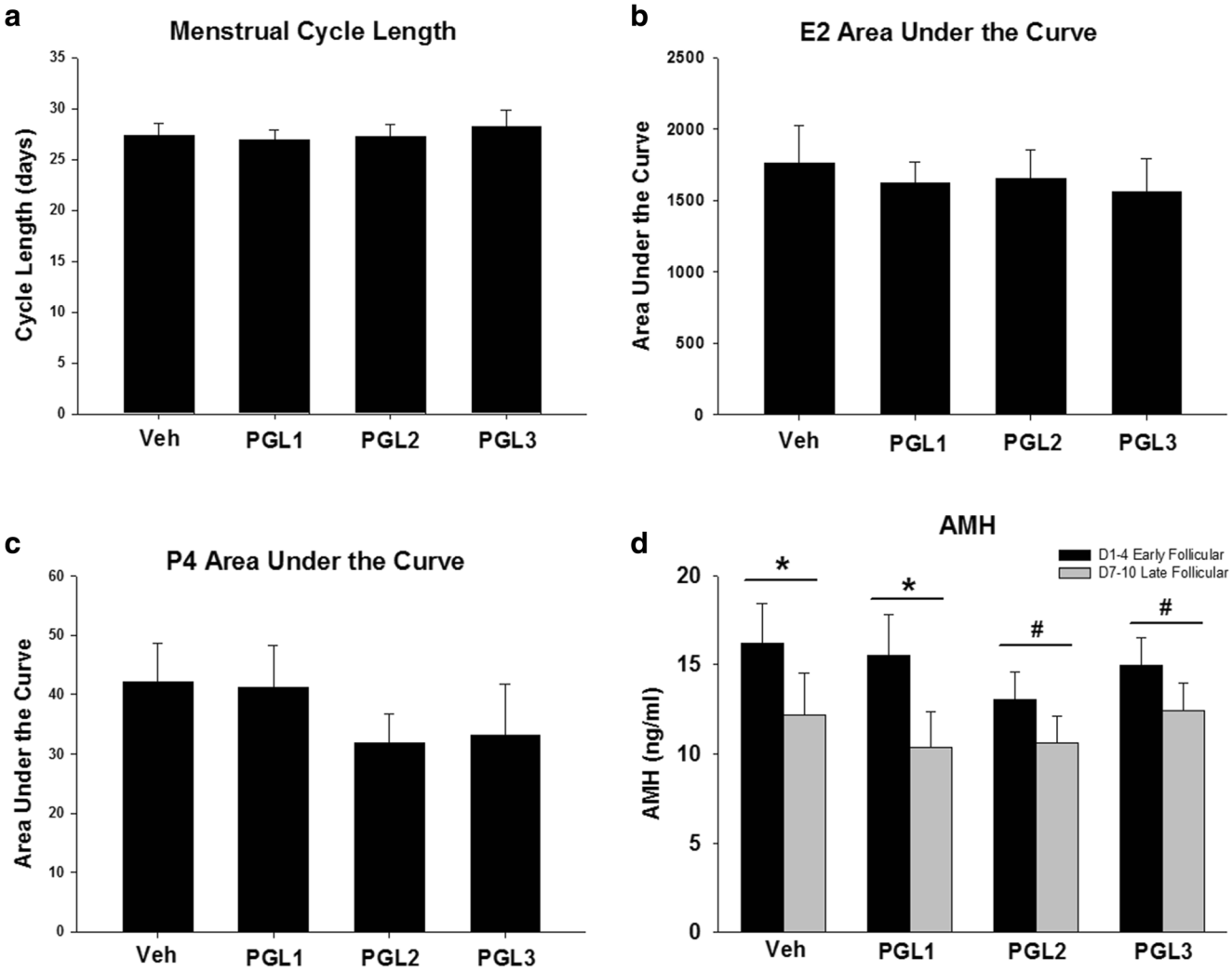

Fig. 2 Menstrual cyclicity and ovarian hormone production during vehicle (Veh) and PGL1001 (PGL) treatment. Length (days) of the menstrual cycle (**a**) as well as area under the curve values for E2 (**b**) and P4 (**c**) was assessed during Veh treatment and through three menstrual cycles of PGL treatment (first treatment cycle = PGL1; second treatment cycle = PGL2; third treatment cycle = PGL3). AMH levels were assessed during the early (D1–4) and late (D7–10) follicular phase of the Veh and each of the PGL treatment menstrual cycles (**d**). Data are presented as mean ± SEM. $^{(*)}$ indicate statistical significance ($p < 0.05$) and $^{(\#)}$ indicate a trend towards statistical significance ($p < 0.1$) between treatment groups

Determination of ovarian size by ultrasound imaging

Ovarian circumference during the early follicular phase increased following one cycle of PGL1001 treatment ($p < 0.05$, Fig. 3a and b) and remained elevated after PGL1001 treatment during the subsequent second and third natural menstrual cycle relative to pretreatment (vehicle) measurements. An increase in size among different treatment cycles was not observed when ovaries were measured during late follicular phase, in which a dominant follicle is often present and occupies a large portion of the ovary (Fig. 3c). While ovarian size was not assessed during each COS cycle, an example of the ovarian ultrasound at the end of a COS cycle is illustrated in Fig. 2d, which demonstrates the presence of multiple follicles in response to exogenous gonadotropins (Fig. 3d).

Controlled ovarian stimulation: hormone production, oocyte maturation, oocyte quantity, and embryonic developmental potential

E2 levels were similar ($p > 0.05$) during the first (vehicle) and second (following PGL1001 treatment) COS cycles (Fig. 4a). However, P4 levels were greater ($p < 0.05$) on D3 (a trend was noted on D6; $p < 0.1$) of the COS protocol in animals treated with PGL1001 (COS2) relative to vehicle-treated animals undergoing a COS protocol (COS1). On D9, 24 h after administration of an ovulatory bolus of hCG, P4 levels were lower ($p < 0.05$) following PGL treatment relative to the P4 values observed during the vehicle COS cycle. D1 and D8 AMH levels remain unchanged ($p > 0.05$) during the COS protocol after vehicle treatment (Fig. 4c). However, following

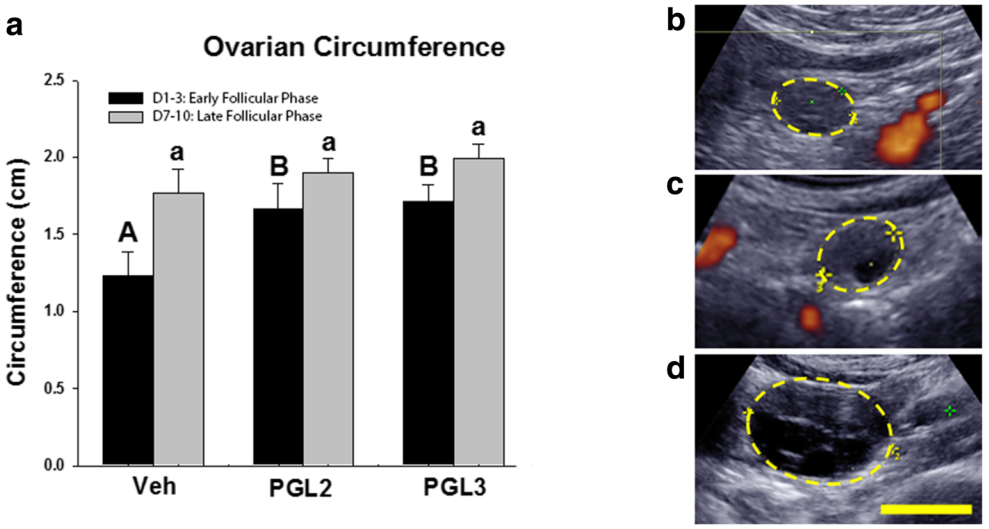

Fig. 3 Ovarian circumference (cm) in natural menstrual cycles after vehicle (Veh) and PGL1001 (PGL) treatment. The size of the ovary was measured by ultrasound (**a**) during the Veh cycle, as well as after one cycle (determined at the beginning of the second PGL cycle, PGL2), two cycles (determined at the beginning of the third PGL cycle, PGL3), and three PGL1001 treatment cycles (determined at the end of the third PGL treatment cycle and just prior to the initiation of the second COS, COS2). Data are presented as mean ± SEM. Different upper and lower case letters represent significant differences ($p < 0.05$) in D1–3 ultrasound (early follicular phase) or D7–10 ultrasound (late follicular phase) measurements between treatment groups, respectively. Ultrasound images of the macaque ovary during early (**b**) and late (**c**) follicular phase as well as during D7–10 of COS cycle (**d**). Scale bar = 1 cm

PGL1001 treatment for three menstrual cycles, D8 AMH levels were elevated ($p < 0.05$) compared to D1 values.

The total number of oocytes retrieved during the COS cycle did not differ ($p > 0.05$) following vehicle or PGL1001 treatment (Fig. 5a). When stratified into different maturational stages (GV, MI, and MII), no difference was observed in the number of GV oocytes obtained following vehicle or PGL1001 treatment. However, the number of MII oocytes was decreased ($p < 0.05$), while there was a trend ($p < 0.1$) for increased numbers of MI oocytes obtained from the COS following PGL1001 treatment relative to the COS protocol performed after vehicle treatment (Fig. 5a). Together, the rate of oocyte maturation remains similar ($p > 0.05$) in COS cycles following vehicle and PGL1001 treatment (Fig. 5c). The numbers of total oocytes retrieved varied among individual animals, reflecting previously reported inter-animal variability [24] and did not correlate with PGL1001 plasma concentration (Supplemental Fig. 1).

Thirty-six hours after IVF, average numbers of 2-cell embryos were 23.8 ± 3.7 and 24.5 ± 4.7 ($p > 0.05$) in COS cycles performed following vehicle and PGL1001 treatment, respectively. Average numbers of uncleaved MII oocytes were 8.8 ± 1.4 and 4.4 ± 1.6 ($p > 0.05$) in COS cycles performed following vehicle and PGL1001 treatment, respectively. Even though the total number of fertilized oocytes were not different in vehicle and PGL1001 treatment cycles, fertilization rate was greater ($p < 0.05$) in oocytes obtained from the COS performed after PGL1001 treatment in comparison to the post-vehicle COS (Fig. 5c). In fact, seven out of eight animals exhibited an increased fertilization rate after PGL1001 treatment compared to the vehicle cycle (Supplemental Fig. 2). Typically, macaque embryos reach the blastocyst stage 7–8 days after fertilization [24]. Embryos that do not progress to blastocysts arrest at an early cleavage stage (2–16 cells) or the morula stage (Fig. 5b) of development. Blastocyst formation rates remain similar ($p > 0.05$) in COS cycles following vehicle and PGL1001 treatment (Fig. 5c).

Discussion

In rodents, SST inhibits primordial follicle activation [16] and blocking the action of SST using an SSTR-2 selective antagonist promotes the transition of follicles from the non-growing into the growing pool [14]. In the current study, we hypothesized that PGL1001, a SSTR-2 antagonist, would also increase ovarian follicle recruitment in a nonhuman primate model (i.e., rhesus macaques), leading to increased number of follicles responsive to gonadotropins and ultimately higher numbers of oocytes retrieved following ovarian stimulation. Female rhesus macaques share similarities with women in terms of reproductive physiology that makes them an excellent preclinical model. Female macaques have a 28-day and mono-ovulatory menstrual cycle, respond similarly to ovarian stimulation, and have comparable IVF and embryonic development outcomes when compared to those observed in women. This is the first report on the ovarian effects and overall safety of long-term (three menstrual cycles) treatment with a SSTR-2 antagonist, PGL1001, in primates. Our results demonstrated that without altering general health or normal

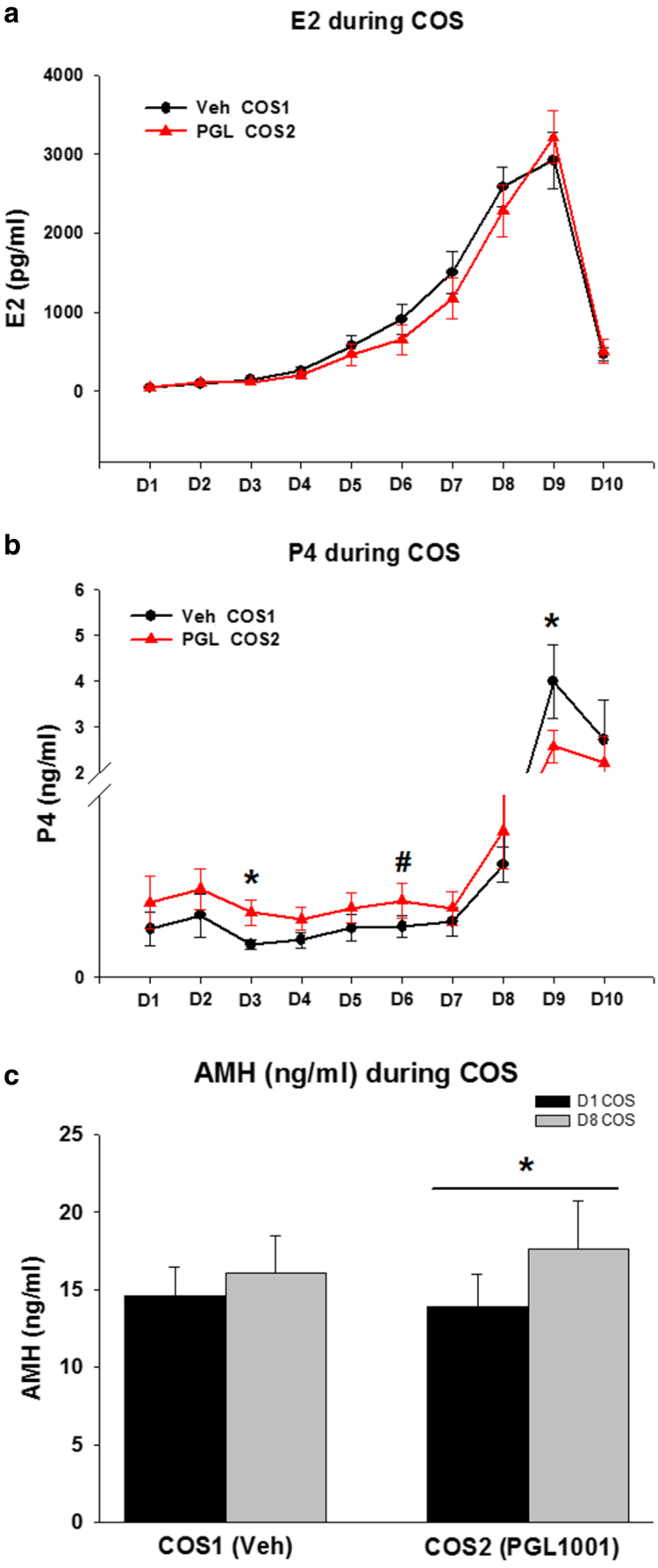

Fig. 4 Circulating steroid levels during controlled ovarian stimulation (COS) protocols following vehicle (Veh; COS1) and three cycles of PGL1001 treatment (PGL; COS2). While daily E2 levels remain similar during COS1 and COS2 (**a**), P4 levels were elevated on days 3, 6, and 9 during the COS protocol that occurred following PGL treatment (**b**). While unchanged in D1 and D8 in COS1, AMH levels were elevated on D8, compared to D1, in COS2 (**c**). Data are presented as mean ± SEM. $^{(*)}$ indicate statistical significance ($p < 0.05$) and $^{(\#)}$ indicate a trend towards statistical significance ($p < 0.1$) between treatment groups

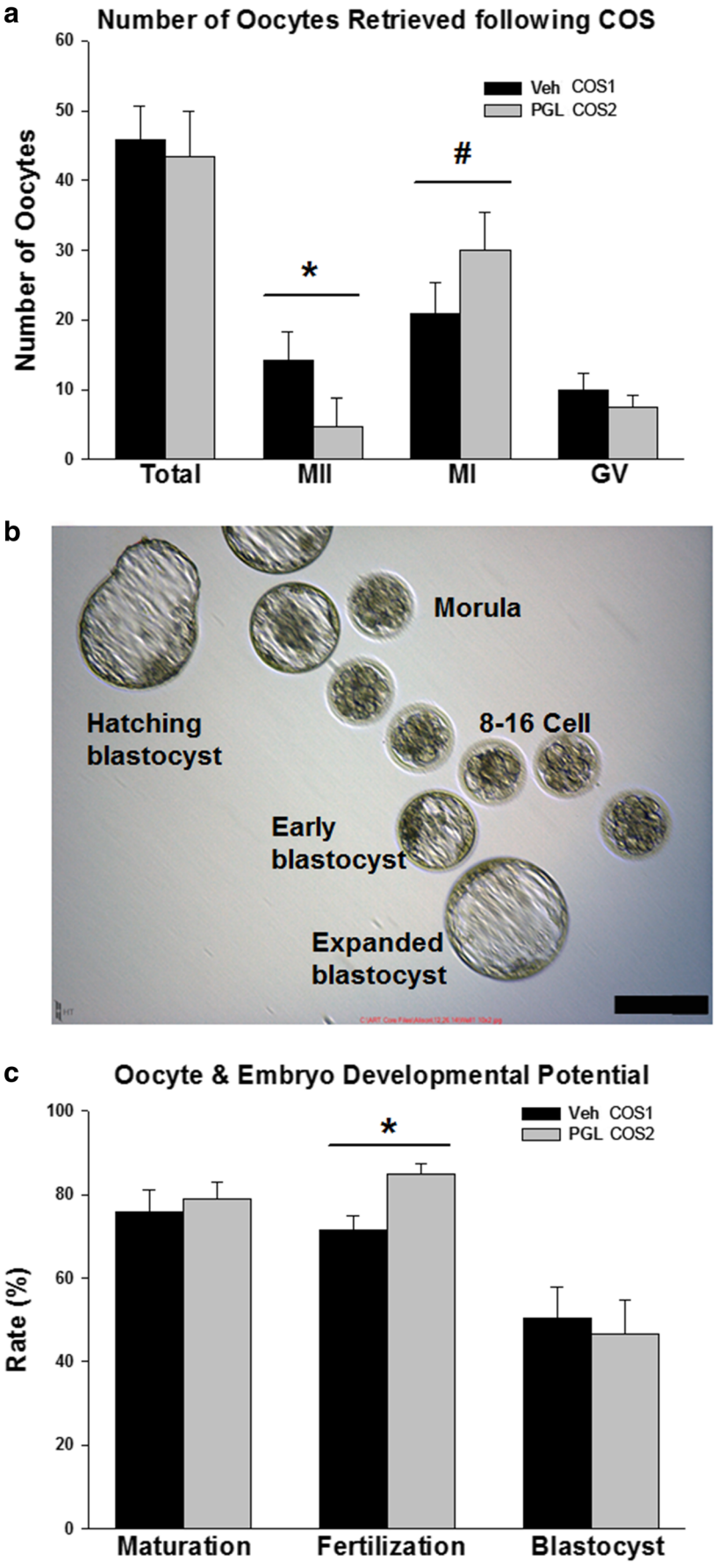

Fig. 5 Oocyte numbers, maturation status, and fertilization/blastocyst development rates following COS protocols performed prior to (vehicle [Veh]) and after three menstrual cycles of PGL1001 (PGL) treatment. **a** While the total numbers of oocytes were similar prior to and after PGL treatment, the mean number of MII oocytes decreased and the number of MI oocytes exhibited an increasing trend after PGL treatment. **b** Representative picture of embryos of different developmental stages on day 8 of culture. Scale bar = 250 μm. **c** Compared to the Veh treatment, maturation and blastocyst formation rates remain similar while the fertilization rate demonstrated a significant increase after PGL treatment. Data are presented as mean ± SEM. $^{(*)}$ indicate statistical significance ($p < 0.05$) and $^{(\#)}$ indicate a trend towards statistical significance ($p < 0.1$) when compared to the Veh treatment groups

menstrual and ovarian steroid hormone pattern, PGL1001 significantly increased the fertilization rate of oocytes obtained following controlled ovarian stimulation (COS). Additional data obtained from this study also indicates that PGL1001 may affect the population of growing follicles.

Circulating PGL1001 accumulated over time, reaching its peak level at the end of the three-cycle treatment and prior to the post-treatment COS. Inter-animal variability of peak PGL1001 levels was observed, although the reason remains unclear. It is recognized that SST is capable of inhibiting the secretion of a variety of exocrine and endocrine hormones or peptides (i.e., growth hormone, thyroid stimulating hormone, gastrointestinal hormones, insulin, and glucagon) [5]. Thus, the potential exists for an SSTR antagonist to exhibit off-target effects. However, PGL1001 did not affect overall animal health and well-being or blood count/chemistry in any of the animals, suggesting that PGL1001 does not significantly impact non-reproductive tissues at the dosage tested in the current study.

PGL1001 also did not alter the length of the natural menstrual cycle or circulating levels of E2, P4, and AMH through three consecutive cycles of treatment compared to the vehicle treatment cycle. All animals exhibited normal follicular and luteal phase length. The E2 peak prior to ovulation as well as the P4 maximum during the luteal phase was not different between vehicle and PGL1001 treatment cycles. AMH is produced by granulosa cells of growing ovarian follicles [28, 29] and its production increases as follicles transition from the preantral to the small antral stage and then decreases as follicles progress to the preovulatory stage [27]. In women, serum AMH level is considered to be a predictor of the size of the growing follicle pool. In the current study, serum AMH during early or late follicular phase did not differ between the vehicle and any of the subsequent PGL1001 treatment cycles. However, AMH levels during the late follicular phase were lower than what was observed during the early follicular phase in the vehicle and the first PGL cycle. A similar trend was observed in the second PGL and third PGL cycles. This reduction could be explained by decreased numbers of small antral follicles as a consequence of dominant follicle selection during the late follicular phase. Interestingly, ovarian circumference during early follicular phase was 36%, 39%, and 50% greater following one, two, and three menstrual cycles of PGL1001 treatment, respectively, relative to the baseline measurement in the vehicle cycle. This modest increase in ovarian size during PGL1001 cycles may be a consequence of prior ovarian stimulation following the vehicle treatment and/or increased follicle recruitment to the growing pool.

During the COS protocols, daily E2 levels were similar between post-vehicle and post-PGL1001 treatments. However, after PGL1001 treatment, P4 serum levels were slightly increased prior to hCG, but decreased after hCG, in comparison to those observed in the vehicle COS cycle. The cause for the differential changes in P4 levels pre- and post-hCG is unclear. Silencing of SSTR-2 expression was reported to increase P4 production in bovine primary granulosa cells by enhancing mRNA levels of steroidogenic acute regulatory protein (STAR) and CYP11A1 without altering aromatase expression or estradiol production [13]. Another study demonstrated that while SST treatment decreased P4 secretion in luteinized human granulosa cells, it stimulated P4 production when treated in combination of hCG [30]. Regardless, the changes in P4 levels during the COS protocol observed in the current study did not correlate with the number of stimulated follicles or oocytes retrieved. Serum AMH levels on days 1 and 8 during COS remain unchanged post-vehicle treatment. AMH levels were significantly elevated on day 8 of the COS protocol performed following three cycles of PGL1001 treatment compared to levels 1 day after the initiation of the COS protocol. In contrast, a significant increase at day 8 versus day 1 of the COS protocol was not observed post-vehicle treatment. It is possible that after PGL1001 treatment, the number of preantral follicles is increased and upon FSH stimulation, they become early/small antral follicles and contribute to higher AMH levels. However, these early/small antral follicles at D8 of COS are potentially too small/immature and thus are not likely to be collected during follicle aspiration.

No difference was observed in the number of total and GV oocytes collected during COS cycles after vehicle and PGL1001 treatment. While this seems to suggest that PGL1001 did not affect the size of the growing follicle pool, it is possible that 3-month PGL1001 treatment promoted primordial-to-preantral follicle growth (increased AMH levels and ovarian size) but did not increase the number of small antral follicles that would contribute to the number of oocyte retrieved following COS. In primates, the time for primordial follicles to reach the antral stage is not well defined. However, it is hypothesized that this time is probably close to 6 months [1, 31]. Interestingly, there seems to be a shift from MII to MI oocytes aspirated from animals following the PGL1001 treatment in comparison to the vehicle treatment. The reason for this shift in oocyte maturation status is presently unclear and requires additional studies. The maintenance of meiotic arrest within oocytes, keeping the oocytes from reaching the mature/MII stage, requires high levels of cAMP [32]. Therefore, it is possible that blocking SSTR-2 signaling increases levels of cAMP, as was demonstrated in cultured granulosa cells [13], which subsequently inhibits the progression towards the MII stage in oocytes. After PGL1001 treatment, the number of oocytes aspirated, as well as oocyte maturation (MII + MI) and blastocyst formation rates, remained similar to what was observed following vehicle treatment. Intriguingly, the fertilization rate, as measured by early embryo cleavage, was

significantly increased in oocytes collected after PGL1001 treatment in comparison to the vehicle cycle. PGL1001, a synthetic peptide, appeared to have a long half-life which accounts for its accumulation and peak circulating value at the end of treatment. Thus, while animals were not treated with PGL1001 during COS, PGL1001 is expected to be present in circulation during the COS cycle. The reason for the increased fertilization rate following PGL1001 treatment is unclear and warrants further investigation.

The COS protocol used in the current study is optimized to collect a maximum number of oocytes per stimulation cycle. In addition, this study employed young female rhesus macaques that are most likely to have a large ovarian reserve. Future studies that include using aging monkeys with limited ovarian reserve may provide insight into whether PGL1001 treatment would increase pregnancy outcomes in women of advanced reproductive age or those with a limited primordial follicle reserve. For example, rhesus macaques with an age range of 14–17 would be appropriate to use as a model similar to women in the age group of 35–43. Similarly, combining PGL1001 treatment with a "milder" COS (i.e., suboptimal gonadotropin treatment) would help establish the ability of an SSTR-2 antagonist to promote the development of greater numbers of preovulatory follicles. Lastly, in the current study, it is unclear whether it is a direct effect of PGL1001 on follicle recruitment, the periovulatory follicle, the cumulus-oocyte complex, or the oocyte itself that promotes fertilization. Thus, the site of action by PGL1001 will also be examined in future studies.

Conclusions

Prolonged treatment of PGL1001 appears to be safe without affecting normal menstrual patterns or ovarian hormone production. In addition, PGL1001 has the potential to improve fertilization rate of oocytes collected following ovarian stimulation. Future studies on mechanisms and the site of PGL1001 action is required to determine possible clinical applications of PGL1001 to improve outcomes of current infertility treatment in Assisted Reproductive Technology.

Acknowledgements We thank Dr. Cecily Bishop for assistance in ultrasound imaging and analysis and Ms. Cathy Ramsey and Dr. Carol Hanna in the ONPRC Assisted Reproductive Technologies (ART) Support Core for assistance in sperm collection, culture media preparation, and in vitro fertilization techniques, as well as Ms. Maralee Lawson and Mr. Nathan Halow for technical assistance. We are also grateful to the ONPRC Endocrine Technology Support and ART Cores (ETSC; NIH P51 OD011092) and the Division of Comparative Medicine, Surgical Services Unit and Clinical Medicine Unit.

Funding This study was supported by NIH (P51 OD011092; JDH) and PregLem SA (JDH).

Compliance with ethical standards

The studies were conducted according to the National Institutes of Health Guide for the Care and Use of Laboratory Animals. All animal protocols and procedures were approved by ONPRC's Institutional Animal Care and Use Committee.

Conflict of interest The authors declare that they have no conflict of interest.

References

1. Gougeon A. Regulation of ovarian follicular development in primates: facts and hypotheses. Endocr Rev. 1996;17(2):121–55.
2. Macklon NS, Fauser BC. Aspects of ovarian follicle development throughout life. Horm Res. 1999;52(4):161–70.
3. Fortune JE, Cushman RA, Wahl CM, Kito S. The primordial to primary follicle transition. Mol Cell Endocrinol. 2000;163(1–2):53–60.
4. Fauser BC, Van Heusden AM. Manipulation of human ovarian function: physiological concepts and clinical consequences. Endocr Rev. 1997;18(1):71–106.
5. Murray PG, Higham CE, Clayton PE. 60 years of neuroendocrinology: the hypothalamo-GH axis: the past 60 years. J Endocrinol. 2015;226(2):T123–40.
6. Hejna M, Schmidinger M, Raderer M. The clinical role of somatostatin analogues as antineoplastic agents: much ado about nothing? Ann Oncol. 2002;13(5):653–68.
7. Narayanan S, Kunz PL. Role of somatostatin analogues in the treatment of neuroendocrine tumors. J Natl Compr Cancer Netw. 2015;13(1):109–17.
8. Rai U, Thrimawithana TR, Valery C, Young SA. Therapeutic uses of somatostatin and its analogues: current view and potential applications. Pharmacol Ther. 2015;152:98–110.
9. Gevers TJ, Drenth JP. Somatostatin analogues for treatment of polycystic liver disease. Curr Opin Gastroenterol. 2011;27(3):294–300.
10. Gambineri A, Patton L, De Iasio R, Cantelli B, Cognini GE, Filicori M, et al. Efficacy of octreotide-LAR in dieting women with abdominal obesity and polycystic ovary syndrome. J Clin Endocrinol Metab. 2005;90(7):3854–62.
11. Gahete MD, Cordoba-Chacon J, Duran-Prado M, Malagon MM, Martinez-Fuentes AJ, Gracia-Navarro F, et al. Somatostatin and its receptors from fish to mammals. Ann N Y Acad Sci. 2010;1200:43–52.
12. Unger N, Ueberberg B, Schulz S, Saeger W, Mann K, Petersenn S. Differential expression of somatostatin receptor subtype 1-5 proteins in numerous human normal tissues. Exp Clin Endocrinol Diabetes. 2012;120(8):482–9.
13. Riaz H, Dong P, Shahzad M, Yang L. Constitutive and follicle-stimulating hormone-induced action of somatostatin receptor-2 on regulation of apoptosis and steroidogenesis in bovine granulosa cells. J Steroid Biochem Mol Biol. 2014;141:150–9.
14. Gougeon A, Delangle A, Arouche N, Stridsberg M, Gotteland JP, Loumaye E. Kit ligand and the somatostatin receptor antagonist, BIM-23627, stimulate in vitro resting follicle growth in the neonatal mouse ovary. Endocrinology. 2010;151(3):1299–309.
15. Nakamura E, Otsuka F, Inagaki K, Tsukamoto N, Ogura-Ochi K, Miyoshi T, et al. Involvement of bone morphogenetic protein activity in somatostatin actions on ovarian steroidogenesis. J Steroid Biochem Mol Biol. 2013;134:67–74.
16. Nestorovic NM, Manojlovic-Stojanoski MN, Trifunovic SL, Ristic NM, Filipovic BR, Sosic-Jurjevic BT, et al. Long-term effects of

somatostatin 14 on the pituitary-ovarian axis in rats. Gen Physiol Biophys. 2014;33(2):157–68.
17. Andreani CL, Lazzarin N, Pierro E, Lanzone A, Mancuso S. Somatostatin action on rat ovarian steroidogenesis. Hum Reprod. 1995;10(8):1968–73.
18. Moaeen-ud-Din M, Malik N, Yang LG. Somatostatin can alter fertility genes expression, oocytes maturation, and embryo development in cattle. Anim Biotechnol. 2009;20(3):144–50.
19. Nestorovic N, Lovren M, Sekulic M, Filipovic B, Milosevic V. Effects of multiple somatostatin treatment on rat gonadotrophic cells and ovaries. Histochem J. 2001;33(11–12):695–702.
20. Phillips KA, Bales KL, Capitanio JP, Conley A, Czoty PW, 't Hart BA, et al. Why primate models matter. Am J Primatol. 2014;76(9):801–27.
21. Wolf DP, Vandevoort CA, Meyer-Haas GR, Zelinski-Wooten MB, Hess DL, Baughman WL, et al. In vitro fertilization and embryo transfer in the rhesus monkey. Biol Reprod. 1989;41(2):335–46.
22. Macklon NS, Stouffer RL, Giudice LC, Fauser BC. The science behind 25 years of ovarian stimulation for in vitro fertilization. Endocr Rev. 2006;27(2):170–207.
23. Wolf DP, Thomson JA, Zelinski-Wooten MB, Stouffer RL. In vitro fertilization-embryo transfer in nonhuman primates: the technique and its applications. Mol Reprod Dev. 1990;27(3):261–80.
24. Hanna CB, Yao S, Ramsey CM, Hennebold JD, Zelinski MB, Jensen JT. Phosphodiesterase 3 (PDE3) inhibition with cilostazol does not block in vivo oocyte maturation in rhesus macaques (Macaca mulatta). Contraception. 2015;91(5):418–22.
25. Bishop CV, Sparman ML, Stanley JE, Bahar A, Zelinski MB, Stouffer RL. Evaluation of antral follicle growth in the macaque ovary during the menstrual cycle and controlled ovarian stimulation by high-resolution ultrasonography. Am J Primatol. 2009;71(5):384–92.
26. Young KA, Hennebold JD, Stouffer RL. Dynamic expression of mRNAs and proteins for matrix metalloproteinases and their tissue inhibitors in the primate corpus luteum during the menstrual cycle. Mol Hum Reprod. 2002;8(9):833–40.
27. Xu J, Bernuci MP, Lawson MS, Yeoman RR, Fisher TE, Zelinski-Wooten MB, et al. Survival, growth, and maturation of secondary follicles from prepubertal, young and older adult, rhesus monkeys during encapsulated three-dimensional (3D) culture: effects of gonadotropins and insulin. Reproduction. 2010.
28. Weenen C, Laven JS, Von Bergh AR, Cranfield M, Groome NP, Visser JA, et al. Anti-Mullerian hormone expression pattern in the human ovary: potential implications for initial and cyclic follicle recruitment. Mol Hum Reprod. 2004;10(2):77–83.
29. Thomas FH, Telfer EE, Fraser HM. Expression of anti-Mullerian hormone protein during early follicular development in the primate ovary in vivo is influenced by suppression of gonadotropin secretion and inhibition of vascular endothelial growth factor. Endocrinology. 2007;148(5):2273–81.
30. Mimuro T, Smith H, Iwashita M, Illingworth PJ. The somatostatin analogue, octreotide, modifies both steroidogenesis and IGFBP-1 secretion in human luteinizing granulosa cells. Hum Reprod. 1998;13(1):150–3.
31. McGee EA, Hsueh AJ. Initial and cyclic recruitment of ovarian follicles. Endocr Rev. 2000;21(2):200–14.
32. Liu L, Kong N, Xia G, Zhang M. Molecular control of oocyte meiotic arrest and resumption. Reprod Fertil Dev. 2013;25(3):463–71.